



UNIVERSITY OF LEEDS

This is a repository copy of *Analysis of substrate binding in individual active sites of bifunctional human ATIC*.

White Rose Research Online URL for this paper:
<http://eprints.whiterose.ac.uk/122681/>

Version: Accepted Version

Article:

Witkowska, D, Cox, HL, Hall, TC et al. (3 more authors) (2018) Analysis of substrate binding in individual active sites of bifunctional human ATIC. *Biochimica et Biophysica Acta (BBA) - Proteins and Proteomics*, 1866 (2). pp. 254-263. ISSN 1570-9639

<https://doi.org/10.1016/j.bbapap.2017.10.005>

© 2017 Elsevier B.V. This manuscript version is made available under the CC-BY-NC-ND 4.0 license <http://creativecommons.org/licenses/by-nc-nd/4.0/>

Reuse

This article is distributed under the terms of the Creative Commons Attribution-NonCommercial-NoDerivs (CC BY-NC-ND) licence. This licence only allows you to download this work and share it with others as long as you credit the authors, but you can't change the article in any way or use it commercially. More information and the full terms of the licence here: <https://creativecommons.org/licenses/>

Takedown

If you consider content in White Rose Research Online to be in breach of UK law, please notify us by emailing eprints@whiterose.ac.uk including the URL of the record and the reason for the withdrawal request.

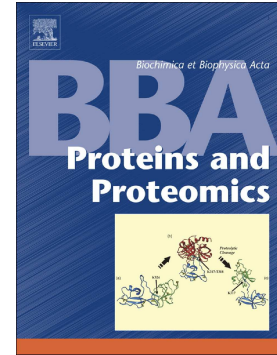


eprints@whiterose.ac.uk
<https://eprints.whiterose.ac.uk/>

Accepted Manuscript

Calorimetric study of substrate binding in individual active sites of bifunctional human ATIC

Danuta Witkowska, Heather L. Cox, Tara C. Hall, Gemma C. Wildsmith, Darren C. Machin, Michael E. Webb



PII: S1570-9639(17)30253-4
DOI: doi:[10.1016/j.bbapap.2017.10.005](https://doi.org/10.1016/j.bbapap.2017.10.005)
Reference: BBAPAP 40028

To appear in:

Received date: 31 May 2017
Revised date: 3 October 2017
Accepted date: 12 October 2017

Please cite this article as: Danuta Witkowska, Heather L. Cox, Tara C. Hall, Gemma C. Wildsmith, Darren C. Machin, Michael E. Webb , Calorimetric study of substrate binding in individual active sites of bifunctional human ATIC. The address for the corresponding author was captured as affiliation for all authors. Please check if appropriate. Bbapap(2017), doi:[10.1016/j.bbapap.2017.10.005](https://doi.org/10.1016/j.bbapap.2017.10.005)

This is a PDF file of an unedited manuscript that has been accepted for publication. As a service to our customers we are providing this early version of the manuscript. The manuscript will undergo copyediting, typesetting, and review of the resulting proof before it is published in its final form. Please note that during the production process errors may be discovered which could affect the content, and all legal disclaimers that apply to the journal pertain.

Calorimetric study of substrate binding in individual active sites of bifunctional human ATIC

Danuta Witkowska, Heather L. Cox, Tara C. Hall, Gemma C. Wildsmith, Darren C. Machin and
Michael E. Webb*

School of Chemistry and Astbury Centre for Structural Molecular Biology, University of Leeds,
LS2 9JT, UK

*Correspondence: m.e.webb@leeds.ac.uk

ABSTRACT

Aminoimidazolecarboxamide ribonucleotide formyl transferase (AICARFT): Inosine monophosphate cyclohydrolase (IMPCH, collectively called ATIC) is a bifunctional enzyme that catalyses the penultimate and final steps in the purine de novo biosynthesis pathway. The bifunctional protein is dimeric and each monomer contains two different active sites both of which are capable of binding nucleotide substrates, this means to a potential total of four distinct binding events might be observed. Within this work we used a combination of site-directed and truncation mutants of ATIC to independently investigate the binding at these two sites using calorimetry. A single S10W mutation is sufficient to block the IMPCH active site allowing investigation of the effects of mutation on ligand binding in the AICARFT active site. The majority of nucleotide ligands bind selectively at one of the two active sites with the exception of xanthosine monophosphate, XMP, which, in addition to binding in both AICARFT and IMPCH active sites, shows evidence for cooperative binding with communication between symmetrically-related active sites in the two IMPCH domains. The AICARFT site is capable of

independently binding both nucleotide and folate substrates with high affinity however no evidence for positive cooperativity in binding could be detected using the model ligands employed in this study.

KEYWORDS: BIFUNCTIONAL ENZYMES, ISOTHERMAL TITRATION CALORIMETRY, MULTIPLE BINDING SITES

ABBREVIATIONS: AICARFT, AICAR transformylase; AMP, adenosine monophosphate; ATIC, 5-aminoimidazole-4-carboxamide ribonucleotide formyl transferase; Inosine monophosphate cyclohydrolase; ATIC WT, ATIC Wild Type; IMPCH, inosine monophosphate cyclohydrolase; ITC, isothermal titration calorimetry; XMP, xanthosine monophosphate.

1. INTRODUCTION

The bifunctional enzyme ATIC (5-aminoimidazole-4-carboxamide ribonucleotide transformylase/Inosine 5'-monophosphate cyclohydrolase) catalyses the final two steps of the de novo purine biosynthetic pathway.¹ This and the corresponding pyrimidine de novo synthesis pathway form one of two methods via which the formation of DNA and RNA nucleotide pools in living cells occurs.² Although the second method, salvage synthesis, has a lower metabolic cost, rapidly-dividing foetal and cancer cells depend mainly on the de novo synthetic pathways and in many tumours there is an absolute dependence for de novo purine biosynthesis.³ Its function in the de novo pathway established ATIC as a target for many anti-inflammatory and antineoplastic agents including: methotrexate, sulfasalazine and pemetrexed.^{4,5} Inhibition of ATIC activity by these anti-folate drugs causes the accumulation of the substrate AICAR (5-aminoimidazole-4-carboxamide ribonucleotide) in cells, activating the cellular energy sensor AMPK (adenosine

monophosphate-activated protein kinase), which briefly speaking suppresses inflammation.⁶ More recently, cyclic peptide inhibitors of ATIC dimerization and small molecules derived from them have been shown to have a similar effect on AMPK.^{7,8} Finally, ATIC and AICAR have recently been implicated in the regulation of the insulin receptor autophosphorylation and its endocytosis.⁹

The 5-aminoimidazole-4-carboxamide ribonucleotide transformylase (AICARFT) and inosine 5'-monophosphate cyclohydrolase (IMPCH) enzymatic activities of ATIC are catalysed by a single purH-encoded bifunctional polypeptide in all organisms apart from the archaea such as *Methanococcus jannaschii*.¹⁰ Structural studies of ATIC enzymes have been conducted on the human,^{11,12} chicken,^{13,14} bacterial¹⁵ and yeast¹⁶ proteins. The overall architectures of the avian and human ATIC are highly homologous as would be expected from their high sequence identity (82%).¹⁷ These structural analyses of the metazoan enzymes have been complemented by a broad range of kinetic, substrate analogue and mutagenesis studies.^{13,18, 19} Truncation mutant studies of human ATIC have shown that the AICARFT and IMPCH activities are encoded on independent domains.¹¹ The AICARFT domain (residues 200–593) is responsible for the transfer of a formyl group from the cofactor N¹⁰-formyl tetrahydrofolate and its polyglutamylated forms to the substrate AICAR producing a stable formylAICAR (FAICAR) intermediate. The smaller N-terminal domain (residues 1–199) has IMPCH activity and catalyzes the cyclization of FAICAR to inosine 5'-monophosphate (IMP)²⁰ (Figure 1a). Structural studies have revealed that ATIC forms an intertwined dimer (Figure 1b), in which the two catalytic sites are separated by approximately 50 Å.^{14,21} Sedimentation equilibrium and dilution experiments show that human PurH apoprotein exists in a monomer:dimer equilibrium mixture with a K_{dim} of 0.55 μM ²² and although the transformylase activity requires dimerization, the monomeric form is sufficient for

the cyclohydrolase activity.²³ Small molecule inhibitors of this dimerization have been reported⁸ and its inhibition in mammalian cells has been tested on obese mouse models.²⁴ It has been shown that inhibition of AICAR transformylase leads to decreasing of elevated blood glucose levels, as well as glucose tolerance improving, and body mass reduction.²⁴

As ATIC is a bifunctional enzyme, previous studies have addressed whether there is a kinetic advantage to this structural organization such as substrate channeling as observed for other multifunctional enzymes.²⁵ However rapid chemical quench, stopped-flow and steady-state kinetics^{26,27,19} all indicate that channelling of FAICAR does not occur with ATIC. In fact, the equilibrium of the AICARFT reaction lies towards AICAR rather than the product.^{28,19} Nevertheless, the higher rate of the IMPCH reaction (36 times faster)²⁸ and the proximity of the AICARFT and IMPCH active sites on ATIC protein appear to be sufficient for capture of FAICAR by IMPCH without channeling or domain-domain communication. Kinetic studies of the purified metazoan enzymes using AICAR together with either 10-formyltetrahydrofolate or the kinetically-preferred 10-formyldihydrofolate²⁸ yield estimates of the apparent Michaelis constants^{11,27} for these substrates in the micromolar range. Using these substrates, Szabados and Christopherson²⁸ investigated the order of ligand binding and proposed that the enzyme proceeds via an ordered mechanism with the tetrahydrofolate substrate binding before AICAR. In this paper, we reinvestigate ligand binding by the enzyme using isothermal titration calorimetry. Via this technique, we hoped to determine whether polyglutamylation of the cofactor would allow us to demonstrate that the ordered binding observed using kinetics measurements could also be observed using equilibrium binding measurements. The two substrate-binding pockets in this enzyme are a confounding variable in these experiments since the AICAR substrate is likely to be able to bind at both the IMPCH and AICARFT active sites and we therefore sought to use

site-directed mutagenesis and truncated protein constructs to deconvolve the signals for ligand binding at each site.

2. MATERIALS AND METHODS

2.1 Materials

Analytical grade reagents were obtained from Sigma Aldrich, Fisher Scientific, Alfa Aesar and VWR International. Water was purified using an ELGA PURLAB® Classic. DNA samples were purified using the Qiagen QIAquick gel extraction kit and Miniprep kit. Molecular biology reagents (including enzymes, plasmids and buffers) were obtained from Promega, Novagen, New England Biolabs, Roche Diagnostics and Invitrogen. Oligonucleotide primers were synthesised by Sigma-Aldrich or IDT. Laboratory plasticware and consumables were supplied by Starlab, Fisher Scientific and Greiner. Kanamycin 1000 x stock at 50 mg/ml was made from kanamycin sulfate (BioChemica). DNA ladder marker Hyperladder I was obtained from New England Biolabs (12 bands, 100 bp-1.5 kbp), the Molecular Weight Marker used in SDS-PAGE gel electrophoresis was obtained from NEB (2-212 kDa) and recombinant DNase 1 from Roche Diagnostics. The resin used in the Ni-NTA column was Qiagen agarose. Vectors pET28a-hATIC and pET28a-aATIC encoding the full-length human and avian isoforms of ATIC were acquired from the Benkovic and Tavassoli laboratories respectively.

2.2 Construction of Truncation and Site-Directed Mutants

DNA MANIPULATION WAS CARRIED OUT USING *E. COLI* DH5A OR *E. COLI* XL10-GOLD FOR DNA AMPLIFICATION. PROTEIN OVEREXPRESSION WAS CONDUCTED USING *E. COLI* BL21 (DE3). SITE-DIRECTED MUTAGENESIS WAS CARRIED OUT VIA QUIKCHANGE MUTAGENESIS USING THE PRIMERS IN TABLE S1 USING PWO DNA POLYMERASE AND AS

OTHERWISE DESCRIBED BY SHIM ET AL.²⁹ WITH THE EXCEPTION OF THE ANNEALING TEMPERATURE THAT WAS ALTERED FROM 65 °C TO 55 °C. PCR SUBCLONING OF ISOLATED DOMAINS INTO PET28A WAS CARRIED OUT USING THE PRIMERS SHOWN IN TABLE S2 USING *Pwo* DNA POLYMERASE WITH 35 CYCLES OF 30 s × 95 °C, 1 MIN × 50 °C (IMPCH) OR 60°C (AICARFT), 2 MIN × 68 °C. DNA WAS PURIFIED USING AND QIAQUICK GEL EXTRACTION KITS (FOR THE TRUNCATION MUTANTS) FOLLOWING THE PROTOCOL SUPPLIED BY THE MANUFACTURER BEFORE RESTRICTION ENZYME DIGESTION AND LIGATION INTO PET28A USING THE SPECIFIED RESTRICTION ENZYMES. LIGATED PLASMIDS WERE PURIFIED BY QIAGEN QIAPREP SPIN MINIPREP AND THE SEQUENCE CONFIRMED BY DIRECT SEQUENCING USING T7FORWARD AND T7TERMINATOR SEQUENCING PRIMERS.

2.3 Protein Expression and Purification

All transformations were carried out under sterile conditions at 4 °C. Plasmids (carrying ATIC or one of its mutants) were transformed to chemically competent *E. coli* BL21(DE3) cells. Starter cultures of LB (5 ml) with kanamycin (50 µg/ml) were inoculated from a single colony from the plates under sterile conditions, and incubated at 37 °C with shaking overnight. The starter cultures were added to auto-induction media (1 L) with kanamycin (final concentration 50 µg/ml) and incubated at 30 °C with shaking overnight. The cells were harvested by centrifugation (JA-10, 8000 rpm, 30 min, 4 °C) and stored at -80 °C. The frozen cell pellet was re-suspended in lysis buffer (1x PBS, 10 mM imidazole) on ice. Recombinant DNase 1 (5,000 units/l) was added to the lysis buffer. The cell suspensions were lysed using the Constant cell disruption system (20 psi, 5 ml injections). Alternatively, the cell suspensions were lysed by sonication (40% power, 4-6 min). The cell debris was sedimented (JA- 25.50, 17000rpm, 40

min) and the supernatant decanted and stored on ice before purification. Ni-NTA resin (~5 ml) was equilibrated with lysis buffer; the lysate loaded and non-binding fractions collected. Lysis buffer (40 ml) followed by this same amount of wash buffer (1xPBS, 50 mM Imidazole) were applied to the column and wash fractions collected. Elution buffer (1x PBS, 250 mM Imidazole) was applied to the column and fractions containing protein (5 ml) were collected. Elution fractions were analysed by SDS-PAGE.

The fractions containing the ATIC protein obtained from the Nickel-affinity column were concentrated to a volume of 1-2 ml via centrifugal concentration (Vivaspin and Amicon) and applied to a 26/60 Superdex 200 gel filtration column using a Pharmacia AKTÄ FPLC system. The purified ATIC was eluted using 50 mM Tris-HCl pH 7.4, 25 mM KCl buffer (called later - ATIC buffer) at a rate of 1.0 ml/min, larger protein fragments being eluted first. Fractions were identified using UV absorbance (280 nm) and SDS-PAGE (using the BioRad tetragel system). ATIC runs as a monomer by SDS-PAGE, which is due to the denaturing conditions of the analysis. The molecular weight (MW) of samples was determined by electrospray ionisation mass spectrometry using a BrukerDaltonics® HCT Ultra™ mass spectrometer and compared to the MW calculated by using Uniprot server (The purification data of ATIC Wild Type (WT) and its mutants are provided in Supplementary section). Protein concentration was calculated by measurement of UV absorption at 280 nm using theoretical extinction coefficients of 54320 M⁻¹ cm⁻¹ (WT), 59820 M⁻¹ cm⁻¹ (S10W mutant) and 7450 M⁻¹ cm⁻¹ (IMPCH domain). FOR THE TRIAL TO REMOVE CO-PURIFIED LIGAND, ALL STEPS WERE CARRIED AS ABOVE UP TO THE PURIFICATION BY NICKEL-AFFINITY COLUMN. AFTER THAT STEP FRACTIONS CONTAINING THE ATIC PROTEIN WERE CONCENTRATED TO A VOLUME OF 2 ML AND DIALYSED FIVE TIMES FOR 12 H AGAINST 1L ATIC BUFFER AT 4 °C.

2.4 ITC studies

A MicroCal™ ITC₂₀₀ (Malvern) was used to carry out the isothermal titration calorimetry studies. Equal buffers were used for the protein and substrate solutions, and the system was maintained at 25 °C. The reference cell was filled with ATIC buffer (~200 µL) or water, and the sample cell filled with a known concentration of protein (~200 µL, 36-79 µM). The titrations were carried out over 20 injections, 1 × 0.5 µL injection followed by 19 × 2.0 µL injections – at a rate of 0.5 µL/s with a recovery time of 120-150 s. The data was fitted using NITPIC, thermodynamic parameters were determined using SEDPHAT, and GUSI was used to present the data.³⁰ In the case of avian ATIC titration by ligands, the data was fitted and thermodynamic parameters were determined using Origin software. Successful determination of the thermodynamic parameters was achieved using a combination of non-linear least-squares fitting, along with selection of an appropriate model which describes the binding interaction under investigation.³¹ In the case of every protein the ITC measurements were carried out one or two days after purification.

3. RESULTS

FULL-LENGTH HUMAN AND AVIAN ATIC WERE OBTAINED VIA BACTERIAL OVEREXPRESSION, AFFINITY PURIFICATION AND SIZE-EXCLUSION CHROMATOGRAPHY. WE INITIALLY USED ISOTHERMAL TITRATION CALORIMETRY TO INVESTIGATE LIGAND BINDING TO THE FULL-LENGTH HUMAN (TABLE 1 AND FIGURES S5-S7 & S10) AND AVIAN ATIC (TABLE S2 AND FIGURE S2-S4). THE FULL-LENGTH PROTEINS ARE ALMOST WHOLLY DIMERIC AT MICROMOLAR CONCENTRATIONS²³ AND EACH MONOMER HAS TWO ACTIVE SITES, IMPCH AND AICARFT. WE INVESTIGATED BINDING OF TWO GROUPS

OF SUBSTRATES: FOLATES AND NUCLEOTIDES. THE FOLATES 10-FORMYLTETRAHYDROFOLATE (10F-THF) AND PTEROYLOLIGOGLUTAMATES (FOLATE OLIGOGLUTAMATE, PTEGLU_N) WERE EXPECTED TO BIND ONLY IN THE AICARFT BINDING POCKET. THE NUCLEOTIDE SUBSTRATES WHICH INCLUDED AICAR, AMP AND XANTHOSINE MONOPHOSPHATE (XMP) WERE EXPECTED TO BIND IN BOTH ACTIVE SITES (STRUCTURES OF ALL LIGANDS ARE SHOWN IN FIGURE 1).

AS EXPECTED, FOR BOTH AVIAN AND HUMAN ATIC, WE OBSERVED NEAR STOICHIOMETRIC BUT WEAK BINDING OF 10-FORMYLTHF AND TIGHT STOICHIOMETRIC BINDING OF BOTH THE CORRESPONDING DI-, AND TRIGLUTAMYLATED OXIDISED COFACTOR. THE FOUR NUCLEOTIDE SUBSTRATES (AICAR, AMP, XMP AND IMP) SHOWED GENERALLY WEAKER BINDING WITH SUB-STOICHIOMETRIC BINDING IN ALL CASES EXCEPT XMP WHICH SHOWED A COMPLEX PATTERN OF BINDING TO MULTIPLE SITES (SEE DISCUSSION BELOW). WE REINVESTIGATED BINDING OF ALL SUBSTRATES USING EXTENSIVELY DIALYSED PROTEIN AND OBSERVED SMALL INCREASES IN THE STOICHIOMETRY OF BINDING FOR MOST OF THESE SUBSTRATES (WITH THE EXCEPTION OF AMP). AT THE SAME TIME, WE OBSERVED A DECREASE IN THE STOICHIOMETRY OF BINDING FOR THE FOLATE COFACTORS SUGGESTING THAT THE OVERALL CONCENTRATION OF BINDING-COMPETENT PROTEIN WAS REDUCED. IN ALL CASES, NO SIGNIFICANT CHANGE IN DISSOCIATION CONSTANT BETWEEN THE DIALYSED AND UNDIALYSED PROTEIN WAS OBSERVED.

ALL TITRATION DATA SETS WERE GLOBALLY FITTED USING A COMBINATION OF NITPIC AND SEDPHAT TO OBTAIN A SINGLE ESTIMATE FOR EACH BINDING PARAMETER FROM MULTIPLE EXPERIMENTS. DATA-PROCESSING USING PRINCIPAL-COMPONENT ANALYSIS

IN NITPIC ENABLES ALMOST USER-INDEPENDENT BASELINE FITTING AND INTEGRATION TOGETHER WITH ASSESSMENT OF THE ERROR IN EACH INTEGRATION DEPENDENT ON THE NOISE IN EACH THERMOGRAM (NOT AVAILABLE BY FITTING IN ORIGIN). FOR MODEL FITTING IN SEDPHAT, EACH BINDING INTERACTION WAS ASSUMED TO BE 1:1 AND THE CONCENTRATION OF PROTEIN CORRECTED BY CALCULATION OF AN 'INCOMPETENT FRACTION' OF THE PROTEIN INCA. THIS IS SUPERFICIALLY SIMILAR TO CALCULATION OF THE NUMBER OF BINDING SITES, N , WHEN FITTING DATA IN ORIGIN. THIS APPROACH ASSUMES THAT THE CONCENTRATION OF THE TITRATED LIGAND IS WELL-DETERMINED (EITHER BY ACCURATE MASS MEASUREMENT OR BY USE OF A KNOWN EXTINCTION COEFFICIENT). ERRORS WERE ESTIMATED BY CALCULATION OF THE 95% CONFIDENCE INTERVAL FOR EACH PARAMETER BASED ON CRITICAL VALUES OF χ^2 . (BRIEFLY, THE PARAMETER UNDER CONSIDERATION IS VARIED AND ALL OTHER PARAMETERS RE-OPTIMISED TO GENERATE χ^2 FOR THAT VALUE, PRODUCING AN EFFECTIVE ERROR SURFACE FOR THAT PARAMETER.) THIS GLOBAL FITTING APPROACH ALSO ENABLES ROBUST ESTIMATION OF ENTHALPY OF BINDING EVEN FOR MODERATE C VALUE EXPERIMENTS ($K_D \approx [\text{PROTEIN}]$) ONLY FOR LOW C-VALUE EXPERIMENTS ($K_D > 10 \times [\text{PROTEIN}]$) WAS IT NOT POSSIBLE TO SIMULTANEOUS FIT BOTH ΔH AND THE INCOMPETENT FRACTION.

THE APPARENT DISSOCIATION CONSTANTS FOR BOTH AICAR ($19 \pm 3 \mu\text{M}$, BASED ON GLOBAL FITTING) AND 10F-THF ($131 \mu\text{M}$, DETERMINED FROM A SINGLE EXPERIMENT) ARE APPROXIMATELY THE SAME AS THE REPORTED MICHAELIS CONSTANTS ($9\text{-}17 \mu\text{M}$ FOR AICAR AND $55\text{-}109 \mu\text{M}$ FOR 10F-THF)^{11,27} WE HAD INITIALLY HOPED THAT THE OCCURRENCE OF ORDERED BINDING WOULD MEAN THAT ONE SUBSTRATE WOULD BIND

MORE WEAKLY IN THE ABSENCE OF THE SECOND SUBSTRATE WHICH WOULD CONFIRM THE FINDINGS OF SZABADOS AND CHRISTOPHERSON.²⁸ GIVEN THE MEASURED DISSOCIATION CONSTANTS THIS IS CLEARLY NOT THE CASE AND BOTH LIGANDS CAN BIND TO THE *APO*-PROTEIN. HOWEVER IN THE CASE OF AICAR BINDING, LESS THAN ONE EQUIVALENT OF AICAR PER PROTEIN MONOMER WAS OBSERVED TO BIND TO THE (UNDIALYSED) PROTEIN (C.F. EXACTLY ONE EQUIVALENT FOR PTEGLU₄); IT IS NOT CLEAR WHETHER THIS CORRESPONDS TO BINDING IN THE IMPCH OR AICARFT ACTIVE SITE. AT THE SAME TIME, MORE THAN A SINGLE EQUIVALENT OF XMP BINDS SUGGESTING THAT THIS MOLECULE, AT LEAST, IS ABLE TO BIND IN BOTH ACTIVE SITES. TO CONFUSE MATTERS FURTHER, CO-PURIFIED NUCLEOTIDES HAVE PREVIOUSLY BEEN OBSERVED IN THE IMPCH ACTIVE SITE AND A REDUCED STOICHIOMETRY OF LIGAND BINDING IS OBSERVED FOR (UNDIALYSED) PROTEIN SAMPLES.¹⁴ AS STATED ABOVE, TO CONTROL FOR THE POSSIBILITY OF CO-PURIFIED LIGANDS, WE REPEATED THE ANALYSIS OF LIGAND BINDING TO FULL-LENGTH HUMAN ATIC AFTER EXTENSIVE DIALYSIS INTO THE BUFFER USED FOR GEL-FILTRATION (FIVE BUFFER CHANGES). IN THESE CASES, THE STOICHIOMETRY OF BINDING FOR AICAR MATCHED THAT FOR THE FOLATE COFACTORS (1:1) SUGGESTING THAT WE HAD DISPLACED CONTAMINATING LIGANDS FROM THE PROTEIN SAMPLE (FIGURE S16). WE ATTEMPTED ANALYSIS OF SMALL MOLECULES PRESENT IN THE BUFFER AFTER THE FIRST DIALYSIS BUT WERE NOT ABLE TO IDENTIFY ANY KNOWN NUCLEOTIDE LIGAND BY MS. IN THE CASE OF AMP A REDUCED STOICHIOMETRY OF BINDING (APPROXIMATELY 0.5 EQUIVALENTS PER MONOMER) WAS OBSERVED – WE THEREFORE INVESTIGATED THE RELATIONSHIP BETWEEN BINDING OF AMP AND AICAR, IN THIS CASE SATURATING CONCENTRATIONS OF AICAR WERE SUFFICIENT TO PREVENT AMP BINDING BUT AICAR BINDING STILL OCCURRED IN THE

PRESENCE OF AMP SUGGESTING THAT THESE BIND AT THE SAME SITE BUT THAT AMP IS ONLY ABLE TO BIND IN ONE SYMMETRICALLY-DISPOSED BINDING SITE IN THE ATIC DIMER (FIGURE S10).

THE THERMODYNAMIC PARAMETERS FOR BOTH NUCLEOTIDE AND FOLATE LIGANDS ARE SIMILAR, IN ALL CASES BINDING OF LIGANDS IS ENTHALPICALLY FAVOURABLE AND ENTROPICALLY UNFAVOURABLE. IN THE CASE OF FOLATE LIGAND SERIES (10FTHF, PTEGLU₂, PTEGLU₃ AND PTEGLU₄), A STEADY INCREASE IN BINDING AFFINITY AS ADDITIONAL γ -GLUTAMYL RESIDUES ARE ADDED TO THE LIGAND IS OBSERVED. THIS IS CONSISTENT WITH THE FORMATION OF ADDITIONAL ELECTROSTATIC INTERACTIONS BETWEEN THE α -CARBOXYL GROUPS OF THE LIGAND AND POSITIVELY CHARGED RESIDUES ON THE PROTEIN SURFACE (OBSERVED AS A STEADY INCREASE IN ΔH). THE ENTROPIC COST OF BINDING ALSO INCREASES AS THE MOLECULE INCREASES IN LENGTH LARGELY DUE TO THE RESTRICTED MOVEMENT OF THE POLYGLUTAMYL TAIL BUT IN ALL CASES THE ENTHALPIC GAIN MORE THAN BALANCES THIS ENTROPIC COST.

THE SHAPE OF THE THERMOGRAM FOR XMP BINDING (WHICH WAS ALSO OBSERVED FOR SAMPLES OF HUMAN AND AVIAN ATIC BEFORE DIALYSIS) IS MORE COMPLEX THAN THAT FOR OTHER LIGANDS AND SUGGESTS THAT AT LEAST 3 DISTINCT BINDING EVENTS OCCUR DURING THE TITRATION, ONE OF WHICH IS ENDOTHERMIC – THE DATA COULD BE FITTED WITH A SEQUENTIAL TERNARY BINDING MODEL TO OBTAIN A SET OF BINDING PARAMETERS (TABLE 1, FIGURE 2c) BUT THE PRESENCE OF THREE BINDING SITES IS INCONSISTENT WITH THE STRUCTURE OF THE PROTEIN AND DETAILED INTERPRETATION OF THE THERMODYNAMIC PARAMETERS UNWISE. TO INVESTIGATE THE RELATIONSHIP BETWEEN XMP AND AICAR BINDING, WE CARRIED OUT A SECOND

TITRATION OF XMP INTO ATIC IN THE PRESENCE OF SATURATING QUANTITIES OF AICAR. THIS GENERATED A SIMPLIFIED TITRATION (FIGURE 2D) CORRESPONDING TO TWO BINDING EVENTS WITH OPPOSITE ENTHALPIES OF BINDING AND DISTINCT BINDING CONSTANTS. THIS DATA COULD BE FITTED WITH BOTH INDEPENDENT AND SEQUENTIAL TWO-SITE BINDING MODELS TO THE PROTEIN DIMER. THE SEQUENTIAL BINDING MODEL YIELDED ESTIMATES FOR THE BINDING ENTHALPY AND DISSOCIATION CONSTANTS CONSISTENT WITH THOSE GENERATED BY THE SEQUENTIAL TERNARY MODEL FOR THE TITRATION OF XMP INTO THE APO-PROTEIN (FIGURE 2 E-G); THIS MODEL IS ALSO MORE PHYSIOLOGICALLY-RELEVANT SINCE THE SYSTEM IS SYMMETRICAL. THE FITTED THERMODYNAMIC PARAMETERS FOR THESE TWO BINDING EVENTS ARE CO-DEPENDENT AND STRONGLY DEPENDENT UPON THE STOICHIOMETRY OF BINDING. IN THIS CASE, WE HAVE ASSUMED A 2:1 BINDING MODEL TO THE PROTEIN DIMER (WITH A 20% INCOMPETENT FRACTION). WHILE THE PRECISE VALUES OF THE THERMODYNAMIC PARAMETERS ARE RELATIVELY POORLY CONSTRAINED DUE TO CO-DEPENDENCE, IT IS CLEAR THAT ONE BINDING EVENT IS EXOTHERMIC, AND ONE ENDOTHERMIC – IN BOTH CASES THE ENTROPY OF BINDING IS POSITIVE (THOUGH THIS MIGHT BE AN ARTEFACT OF UNDERESTIMATING ΔH) BUT INCREASES FOR THE SECOND BINDING EVENT TO COMPENSATE FOR THE SWITCH FROM AN EXOTHERMIC TO ENDOTHERMIC BINDING EVENT.

WE HYPOTHESE THAT WHILE BINDING OF XMP IN ONE MONOMER OF THE PROTEIN DIMER IS ENTHALPICALLY FAVOURABLE, SUBSEQUENT BINDING IN THE SYMMETRICALLY DISPOSED SITE IS ENTHALPICALLY UNFAVOURABLE AS A RESULT OF THE FIRST BINDING EVENT. FROM THE DATA OBTAINED IT IS NOT CLEAR WHETHER THIS SITE IS THE IMPCH OR AICARFT ACTIVE SITE HOWEVER THE IMPCH SITES ARE

CLOSELY PLACED IN SPACE AND NEGATIVE COOPERATIVITY OF THIS TYPE IS CONSISTENT WITH THE OBSERVATIONS OF WOLAN AND CO-WORKERS.¹² IN THEIR CRYSTAL STRUCTURES, THEY OBSERVED 50% BINDING OF XMP IN THE IMPCH ACTIVE SITE AND OCCUPANCY OF THE SECOND SITE ONLY AT HIGHER CONCENTRATIONS OF THE NUCLEOTIDE ACCOMPANIED BY SIGNIFICANT DISTORTIONS IN THE LIGAND. THIS IS POSSIBLE OVERALL BECAUSE OF A LARGE ENTROPIC BENEFIT DUE TO DESOLVATION OF THE PREORGANISED BINDING SITE FOR THE SECOND LIGAND. IN THE CASE OF THE XMP TITRATION INTO THE *APO*-ENZYME, WE ARE OBSERVING BINDING IN ALL FOUR SITES WITH SEQUENTIAL BINDING INTO THE IMPCH ACTIVE SITE AND BINDING INTO THE TWO AVAILABLE AICARFT SITES OCCURRING SIMULTANEOUSLY. FOR THE DIALYSED PROTEIN SAMPLE, THIS YIELDS THE OVERALL COMPLEX CURVE SHAPE, WITH AN OVERALL STOICHIOMETRY OF APPROXIMATELY 1.6:1 (I.E. 20% INCOMPETENT PROTEIN FRACTION) CONSISTENT WITH THE APPARENT STOICHIOMETRY OF 0.8 OBSERVED FOR EITHER AICAR OR FOLATE COFACTORS. GIVEN THIS OBSERVATION, WE HYPOTHESESE THAT THE OBSERVED AICAR BINDING IS AT THE AICARFT SITE, WHEREAS WE OBSERVE XMP BINDING IN BOTH SITES WITH THE CLOSE PROXIMITY OF THE TWO NUCLEOTIDE BINDING SITES IN THE IMPCH DOMAIN DIMER LEADING TO THE DETECTED NEGATIVE COOPERATIVITY.

To confirm that AICAR binding occurs at the AICARFT site rather than the IMPCH site we sought to generate the isolated IMPCH and AICARFT domains. As previously noted, AICARFT requires dimerization for activity but IMPCH does not. A large proportion of the dimerization interface is an interdigitated eight-stranded β -sheet lying between the two catalytic domains. Due to this need for dimerization for binding in the AICARFT binding site we initially retained this motif in the construct for AICARFT and two constructs encoding residues 1-200 and 201-592

were subcloned into pET28a to generate N-terminally His-tagged constructs. Expression trials revealed strong overexpression for the IMPCH construct (residues 1-200) but not for the AICARFT construct (residues 201-592). Overexpression and purification of the IMPCH protein on large scale yielded dimeric protein (based on an estimated MW of 48 kDa from size-exclusion chromatography) consistent with the observations of Anderson et al.²² We investigated the folding of this protein and the effect of ligand binding on the protein using differential scanning fluorimetry (see Figure S1). While binding of both IMP and AICAR stabilized the IMPCH domain in a dose-dependent manner ($\Delta T_m \sim 9^\circ\text{C}$), addition of AMP showed a much smaller dose-independent response ($\Delta T_m \sim 3^\circ\text{C}$). We then repeated the ITC analysis of ligand binding to this protein (see Table 2, and Figure S15), observing binding of three out of four nucleotides (AMP did not bind consistent with the DSF results) and we observed no interaction with the polyglutamylated PteGlu₄ as expected. In two cases, the binding of the nucleotides was marginally weaker than observed for the complete protein but was still sub-stoichiometric, in the case of IMP tighter binding was observed. This appears to conflict with our interpretation of interaction with the full-length protein since AICAR appears to bind in the IMPCH active site and we do not observe negative cooperativity in the XMP binding.

Since we were unable to overexpress the AICARFT domain alone, we instead mutated the IMPCH active-site in the full-length protein in order to block ligand binding. A single S10W mutation in which the indole ring of the inserted tryptophan residue is projected into the nucleobase binding pocket leads to a protein with a slightly lower dissociation constant for both AICAR and PteGlu₄ (Table 3 and Figure 3). In summary, while the isolated IMPCH domain appears to bind AICAR with lower affinity than the intact protein, mutation of the IMPCH site in the full-length protein leads to apparent tighter binding of AICAR. This suggests that AICAR

binds at the AICARFT active site not in the IMPCH active site and that binding of AICAR by the isolated IMPCH domain is not physiologically relevant. This is likely to be due to the smaller dimerization interface in the protein leading to greater permissiveness of binding in the IMPCH site resulting in loss of communication between the two sites.

We had originally hypothesized that the S10W mutation would block AICAR binding in the IMPCH active site. We therefore used this mutation to investigate the effect of binding of the nucleotide and folate ligands in the AICARFT active site and carried out sequential pairwise titration of the two ligands into both WT protein and the S10W mutant protein (Figures 3a, 3b and S9 and S13). In both cases, addition of PteGlu₄ partially inhibited binding of AICAR (Table 3). This inhibition suggests that binding of the fully oxidised folate cofactor perturbs binding of AICAR, supporting the hypothesis that the observed binding of AICAR is in the AICARFT active site. In this case we are using a model ligand for one substrate and the subtle conformation change in the pteridine ring relative to the dehydropteridine ring or tetrahydropteridine ring observed in the substrate may be sufficient to sterically prevent simultaneous binding of the AICAR and PteGlu₄ ligands in their preferred conformations. Alternatively, the binding of both ligands in the Michaelis complex may be negatively cooperative – based on this pair of ligands it is not possible to unambiguously distinguish these possibilities.

AICAR interacts with the AICARFT active-site via a large number of hydrogen-bonding and charge-charge interactions. To unambiguously confirm that the AICAR binding observed was in this site, we investigated the effect of mutation of Phe590 upon binding of the ligand – the side chain of this residue forms a T-shaped π - π interaction with the imidazole ring of AICAR and removal of this interaction would be expected to lead to a small but measurable change in binding affinity. We generated two S10W-F590I and S10W-F590A double mutants and

investigated the effect of the additional mutation on binding of AICAR, PteGlu₄ and AICAR in the presence of 100 μ M PteGlu₄ (Table 3, Figures 4 and S14). For both mutants, we observed no significant change in the affinity for PteGlu₄ but a reduced affinity for AICAR. In this case, the reduced affinity for AICAR meant that we were not able to observe binding of AICAR in the presence of PteGlu₄. This is consistent with this small molecule not being capable of competing with the tighter binding competitor ligand and conclusively demonstrates that the observed AICAR binding is at the AICARFT site and not at the IMPCH active site.

4. Discussion

In this study we originally sought to use calorimetry to investigate ligand binding in the AICAR formyltransferase active site. Previous kinetic studies suggest that ordered ligand binding occurs during catalysis with the folate cofactor binding first.^{1,28} In all of these studies, the non-physiological 10-formyltetrahydrofolate or 10-formyldihydrofolate cofactor is used.²⁹ As shown by our calorimetric analysis, these bind with approximately 600-fold lower affinity than the oxidised form of the physiological product (folyl-triglutamate, PteGlu₄). In our analysis, we are able to see binding of both substrates (10-fTHF and AICAR) to the apo-protein. Initially it was not possible to determine at which site (IMPCH or AICAR Tfase) the substrate AICAR binds but experiments using the variant protein supported the notion that binding was occurring at the AICAR Tfase active site, since a mutation in the IMPCH active site had little effect (actually a small apparent increase in affinity) but mutation in the AICAR Tfase site reduced binding significantly. Binding of ligands in this site has previously been shown to be dependent upon protein dimerization and it is therefore possible that the S10W mutation stabilizes this multimerization slightly increasing the protein dimerization.

AICAR, AMP and XMP exhibit distinct binding preferences – with AMP and AICAR binding solely in the AICAR Tfase active site and XMP binding in both active sites. The most striking feature of this analysis is the negative cooperativity observed for binding of XMP in the IMPCH active site. In their crystal structure of 1m9n, Wolan et al. modelled the electron density in both IMPCH active sites (for both monomers) as two conformationally-distinct XMP molecules, showing that the C2 carbonyl in one of these molecules is held in a planar conformation but in the second the C2 carbonyl is bent out of the plane by $\sim 20^\circ$.¹² This distortion led the authors to suggest that under physiological conditions, half-the-sites reactivity may be occurring in the IMPCH active sites of ATIC.¹² Our calorimetric analysis provides preliminary supporting analysis for this hypothesis since while binding of one molecule is enthalpically favourable, binding of the second is not consistent with the observed distortion. The lower binding stoichiometry of IMP supports this hypothesis – an amino group in this position cannot be sufficiently distorted to permit binding. This limitation appears to be released in the isolated IMPCH domain, with loss of negative cooperativity for XMP and an increased stoichiometry of binding for IMP suggesting that the eight-stranded β -sheet C-terminal to the IMPCH domain is critical to this regulatory communication. It is also possible that binding of XMP has a regulatory role – tight binding of XMP in one active site may be sufficient to inhibit binding of formyl AICAR in the second active site or catalysis of cyclisation. Since XMP is the intermediate between the pathway to GMP from the product IMP this could provide a regulatory role.

It is clear that the AICAR Tfase active site can bind either substrate first. If the reported ordered binding mechanism of Szabados and Christopherson²⁷ is correct then the Enzyme-AICAR complex is not catalytically competent. We had hoped that patterns of enhanced or inhibited second substrate binding would reveal cooperativity in binding but our analysis indicates that

binding of AICAR and the oxidised co-factor in their favoured geometries are mutually exclusive preventing confirmation of cooperative binding using these substrates and calorimetry. Such an analysis would still be possible using the singly reduced dihydrofolyl triglutamate were this to be produced. The strong binding of the oxidised cofactor also highlights the importance of maintaining the cellular pool of reduced folate cofactors and suggests an additional, indirect cellular mode of action for the antifolate inhibitors of dihydrofolate reductase.

4.1 Conclusion

That work shows the first attempt to characterise ligand binding by human ATIC using calorimetry. This analysis was complicated by the presence of multiple, distinct binding sites, however for the majority of ligands it is possible to use a combination of site-directed mutagenesis and competition experiments to identify the binding site and decompose the binding process. Despite the many detailed structural analysis of this enzyme already reported, this study further proves that this complex dimeric enzyme has many more hidden intricacies to be revealed.

AUTHOR CONTRIBUTIONS

D.W., H.L.C., T.C.H., D.C.M. and G.W. carried out mutagenesis and construct preparation.

H.L.C. carried out ITC analysis of ligand binding to avian ATIC and the isolated IMPCH domain. D.W. carried out analysis of ligand binding to human ATIC, S10W and double mutants.

D.W., H.L.C. and M.E.W. designed the project, analysed data and wrote the paper.

FUNDING SOURCES

This project has received funding from the European Union's Horizon 2020 research and innovation programme under the Marie Skłodowska-Curie grant agreement No 657978. HLC was supported by an EPSRC DTA studentship from the University of Leeds. DCM was supported by a BBSRC CASE award BB/K501049/1. GW is supported by BBSRC funding BB/L001551/1.

Acknowledgement

We would like to acknowledge valuable technical discussions with Iain Manfield and Bruce Turnbull.

Figure Captions

Figure 1. a) Catalytic activity of ATIC. Aminoimidazolecarboxamide ribonucleotide (AICAR) is transformed into formyl-aminoimidazolecarboxamide ribonucleotide (fAICAR) using either a 10-formyltetrahydrofolate or 10-formyldihydrofolate cofactor. In vivo the cofactors are poly- γ -glutamylated. fAICAR is subsequently cyclised to form inosine monophosphate (IMP). b) Structure of human ATIC (1pkx) showing the intertwined dimeric structure. XMP is shown bound in the IMPCH active site (red, left). The AICARFT active site is adjacent to the potassium binding site (purple, right). Molecular graphics and analyses were performed with the UCSF Chimera package.¹ c) Structures of ligands used for ITC calorimetric experiments in this study.

Figure 2. ITC thermograms for ligands binding to full-length human ATIC after exhaustive dialysis a) AICAR b) PteGlu₄ and c) XMP binding to human ATIC, d) XMP binding to human ATIC in the presence of 1.1 equivalents of AICAR (saturating concentration), e) full binding model required to explain binding of XMP to full-length ATIC at four sites, f) empirical model used to fit of thermogram c suggesting that one pair of symmetrically disposed binding sites are independent whereas two show negative cooperativity. i.e. $K_d^1 = K_d^{0n/1n}$, $K_d^2 = K_d^{1n/2n}$ and $K_d^3 = K_d^{n0/n1} = K_d^{n1/n2}$, g) binding model used to fit binding of XMP in the presence of saturating AICAR. Derived dissociation constants are within error of the equivalent parameters in empirical model f.

Figure 3. ITC thermograms for AICAR binding to a) full-length ATIC, b) ATIC-S10W and c) isolated IMPCH domain. All titrations were carried out at the 25°C. d) Structure of the IMPCH active site with XMP bound (1m9n), showing relationship between lysine residues and the phosphate group of the substrate and the position of Ser10 relative to the purine ring of the substrate. We hypothesized the indole ring in a S10W mutant would fill this pocket.

Figure 4. ITC thermograms for a. AICAR binding to full-length ATIC-S10W in the presence of 100 μ M PteGlu₄, b. AICAR binding to full-length ATIC-S10W/F590I and c. AICAR binding to ATIC-S10W/F590A in the presence of 100 μ M PteGlu₄ showing complete loss of binding. d. Structure of the AICAR Tfase active site with AICAR bound (1m9n), showing relationship between mutated Phe590 and the imidazole base of AICAR. Loss of this T-shaped π - π interaction is sufficient to prevent effective competition between PteGlu₄ and AICAR for binding to the active site.

TABLE CAPTIONS

Table 1. Results of global fitting of small molecule binding to full-length human ATIC analysed by isothermal titration calorimetry – no changes in affinity occur as a result . All titrations were carried out at 25 °C with protein concentrations of 70-77 μ M and small molecule concentrations in the range 1-1.5 mM. *NB The magnitude of the fitted binding parameters for XMP binding are strongly co-dependent and dependent upon the assumed binding model. These are included for indicative purposes only. n = number of repeat experiments used for global fitting

Table 2. Result of small molecule binding to IMPCH mutant of ATIC protein. All titrations were carried out at 25 °C (single titrations)

Table 3. Calculated parameters for binding of AICAR and PteGlu₄ to the ATIC-WT and ATIC-S10W site-directed mutants. All experiments were carried out at 25°C. The concentration of proteins was in a range 58-77 μ M, concentration of AICAR and PteGlu₄ 1 mM.

REFERENCES

-
- [1] W.T. Mueller, S.J. Benkovic, On the purification and mechanism of action of 5-aminoimidazole-4-carboxamide-ribonucleotide transformylase from chicken liver, *Biochemistry* 20 (1981) 337-344.
- [2] A.N. Lane, T.W.-M. Fan, Regulation of mammalian nucleotide metabolism and biosynthesis, *Nucleic Acids Res.* 43 (2015) 2466-2485.
- [3] X. Tong, F. Zhao, C.B. Thompson, The molecular determinants of de novo nucleotide biosynthesis in cancer cells, *Curr. Opin. Genet. Dev.* 19 (2009) 32–37.
- [4] R.I. Christopherson, S.D. Lyons, P.K. Wilson, Inhibitors of de novo nucleotide biosynthesis as a drugs, *Acc. Chem. Res.* 35 (2002) 961-971.
- [5] Y. Wang, S. Mitchell-Ryan, S. Raghavan, C. George, S. Orr, Z. Hou, L.H. Matherly, A. Gangjee, Novel 5-Substituted Pyrrolo[2,3-d]pyrimidines as Dual Inhibitors of Glycinamide Ribonucleotide Formyltransferase and 5-Aminoimidazole-4-carboxamide Ribonucleotide Formyltransferase and as Potential Antitumor Agents, *J. Med. Chem.* 58 (2015) 1479-1493.
- [6] B.N. Cronstein, M.A. Eberle, H.E. Gruber, R.I. Levin, Methotrexate inhibits neutrophil function by stimulating adenosine release from connective tissue cells, *Proc. Nat. Acad. Sci. USA* 88 (1991) 2441-2445.
- [7] A. Tavassoli, S.J. Benkovic, Genetically Selected Cyclic-Peptide Inhibitors of AICAR Transformylase Homodimerization, *Angew. Chem. Int. Ed.* 44 (2005) 2760–2763.
- [8] I.B. Spurr, C.N. Birts, F. Cuda, S.J. Benkovic, J.P. Blaydes, A. Tavassoli, Targeting tumour proliferation with a small-molecule inhibitor of AICAR transformylase homodimerization, *Chembiochem* 13 (2012) 1628–1634.
- [9] M. Boutchueng-Djidjou, G. Collard-Simard, S. Fortier, S.S. Hébert, I. Kelly, C.R. Landry, L.R. Faure, The Last Enzyme of the De Novo Purine Synthesis Pathway 5-aminoimidazole-4-carboxamide Ribonucleotide Formyltransferase/IMP Cyclohydrolase (ATIC) Plays a Central Role in Insulin Signaling and the Golgi/Endosomes Protein Network, *Mol. Cell. Proteomics* 14 (2015) 1079-1092.
- [10] M. Graupner, H. Xu, R.H. White, New class of IMP cyclohydrolase in *Methanococcus jannaschii*, *J. Bacteriol.* 184 (2002) 1471-1473.
- [11] E.A. Rayl, B.A. Moroson, G.P. Beardsley, The human purH gene product, 5-aminoimidazole-4-carboxamide ribonucleotide formyltransferase/IMP cyclohydrolase. Cloning, sequencing, expression, purification, kinetic analysis, and domain mapping, *J. Biol. Chem.* 271 (1996) 2225-2233.

- [12] D.W. Wolan, C.G. Cheong, S.E. Greasley, I.A. Wilson, Structural Insights into the Human and Avian IMP Cyclohydrolase Mechanism via Crystal Structures with the Bound XMP Inhibitor, *Biochemistry* 43 (2004) 1171–1183.
- [13] L. Ni, K.Guan, H. Zalkin, J.E. Dixon, De novo purine nucleotide biosynthesis: cloning, sequencing and expression of a chicken PurH cDNA encoding 5-aminoimidazole-4-carboxamide- ribonucleotide transformylase-IMP cyclohydrolase, *Gene* 106 (1991) 197-205.
- [14] S.E. Greasley, P. Horton, J. Ramcharan, G.P. Beardsley, S.J. Benkovic, I.A. Wilson, Crystal structure of a bifunctional transformylase and cyclohydrolase enzyme in purine biosynthesis, *Nat.Struct. Biol.* 8 (2001) 402–406.
- [15] J. Le Nours, E.M. Bulloch, Z. Zhang, D.R. Greenwood, M.J. Middleditch, J.M. Dickson, E.N. Baker, Structural Analyses of a Purine Biosynthetic Enzyme from *Mycobacterium tuberculosis* Reveal a Novel Bound Nucleotide, *J. Biol. Chem.* 286 (2011) 40706-40716.
- [16] A.S. Tibbetts, D.R. Appling, Characterization of Two 5-Aminoimidazole-4-carboxamide Ribonucleotide Transformylase/Inosine Monophosphate Cyclohydrolase Isozymes from *Saccharomyces cerevisiae*, *J. Biol. Chem.* 275 (2000) 20920–20927.
- [17] G.C Cheong, D.W. Wolan, S.E. Greasley, P.A. Horton, G.P. Beardsley, I.A. Wilson, Crystal structures of human bifunctional enzyme aminoimidazole-4-carboxamide ribonucleotide transformylase/ IMP cyclohydrolase in complex with potent sulfonyl-containing antifolates. *J. Biol. Chem.* 279 (2004) 18034–18045.
- [18] J.M. Vergis, G.P. Beardsley, Catalytic Mechanism of the Cyclohydrolase Activity of Human Aminoimidazole Carboxamide Ribonucleotide Formyltransferase/Inosine Monophosphate Cyclohydrolase, *Biochemistry* 43 (2004) 1184–1192.
- [19] M. Wall, J.H. Shim, S.J. Benkovic, Human AICAR Transformylase: Role of the 4-Carboxamide of AICAR in Binding and Catalysis, *Biochemistry* 39 (2000) 11303–11311.
- [20] D.W. Wolan, S.E. Greasley, G.P. Beardsley, I.A. Wilson, Structural insights into the avian AICAR transformylase mechanism, *Biochemistry* 41 (2002) 15505-15513.
- [21] D.A. Wolan, S.E. Greasley, M.J. Wall, S.J. Benkovic, I.A. Wilson, Structure of avian AICAR transformylase with a multisubstrate adduct inhibitor beta-DADF identifies the folate binding site, *Biochemistry* 42(37) (2003) 10904-14.
- [22] G.P. Beardsley, E.A. Rayl, K. Gunn, B.A. Moroson, H. Seow, K.S. Anderson, J. Vergis, K. Fleming, S. Worland, B. Condon, J. Davies, Structure and functional relationships in human pur H, *Adv. Exp. Med. Biol.* 431 (1998) 221–226.

- [23] J.M. Vergis, K.G. Bullock, K.G. Fleming, G.P. Beardsley, Human 5-aminoimidazole-4-carboxamide ribonucleotide transformylase/inosine 5'-monophosphate cyclohydrolase. A bifunctional protein requiring dimerization for transformylase activity but not for cyclohydrolase activity, *J. Biol. Chem.* 276 (2001) 7727–7733.
- [24] D.J. Asby, F. Cuda, M. Beyaert, F.D. Houghton, F.R. Cagampang, A. Tavassoli, AMPK Activation via Modulation of De Novo Purine Biosynthesis with an Inhibitor of ATIC Homodimerization, *Chem. Biol.* 22 (2015) 838–848.
- [25] H.O. Spivey, J. Ovadi, Substrate channelling, *METHODS* 19 (1999) 306–321.
- [26] K.G. Bullock, G.P. Beardsley, K.S. Anderson, The kinetic mechanism of the human bifunctional enzyme ATIC (5-amino-4-imidazolecarboxamide ribonucleotide transformylase/inosine 5'-monophosphate cyclohydrolase). A surprising lack of substrate channeling, *J. Biol. Chem.* 277 (2002) 22168-22174.
- [27] E. Szabados, R.I. Christopherson, Relationship between the catalytic sites of human bifunctional IMP synthase, *Int. J. Biochem. Cell. Biol.* 30 (1998) 933–942.
- [28] J.E. Baggott, T. Tamura, Folate-Dependent Purine Nucleotide Biosynthesis in Humans, *Adv. Nutr.* 6, (2015) 564-71.
- [29] J.H. Shim, M. Wall, S.J. Benkovic, N. Diaz, D. Suarez, K.M. Merz, Evaluation of the Catalytic Mechanism of AICAR Transformylase by pH-Dependent Kinetics, Mutagenesis, and Quantum Chemical Calculations, *JACS* 123 (2001) 4687-4696.
- [30] S. Keller, C. Vargas, H. Zhao, G. Piszczek, C.A. Brautigam, P. Schuck, High-Precision Isothermal Titration Calorimetry with automated peak-shape analysis, *Anal Chem* 84 (2012) 5066-5073.
- [31] W.B. Turnbull, A.H. Daranas, On the Value of c : Can Low Affinity Systems be studied by Isothermal Titration Calorimetry? *JACS* 125 (2003) 14859-14866.

Figure 1

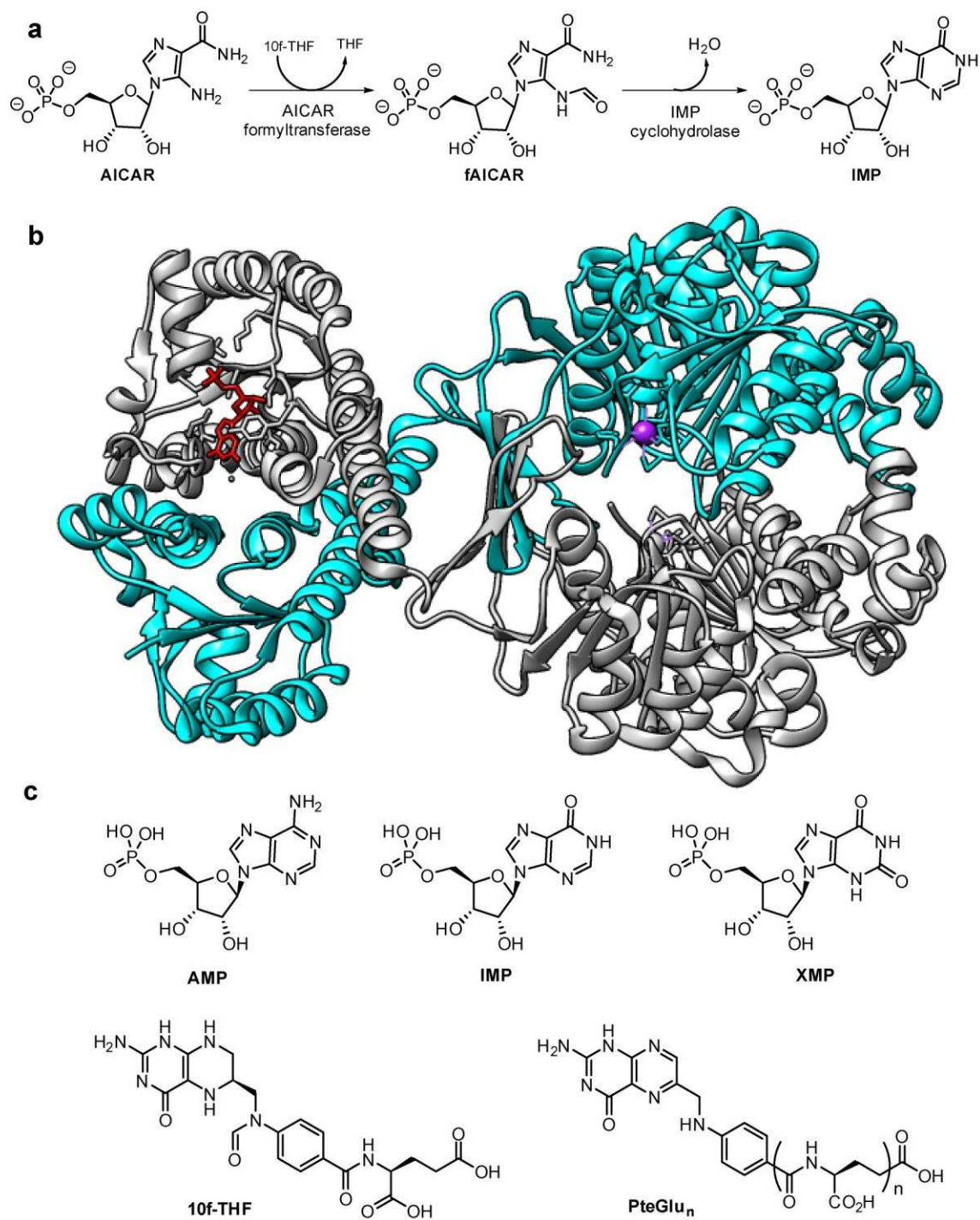


Figure 2

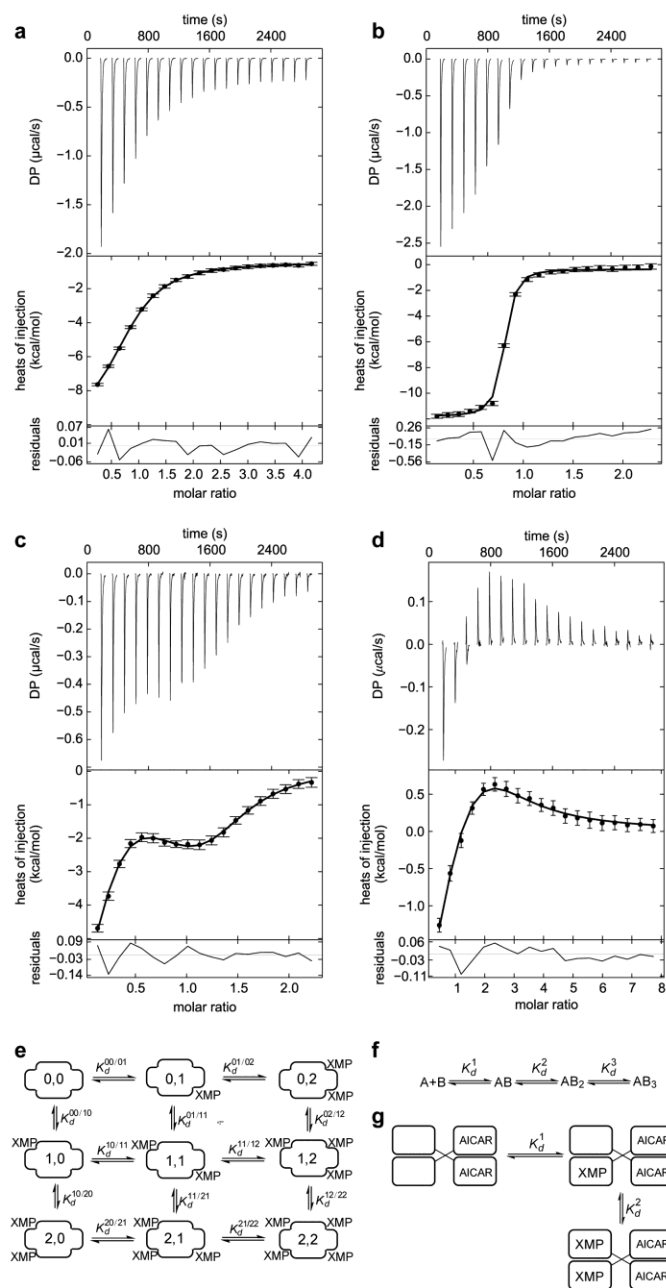


Figure 3

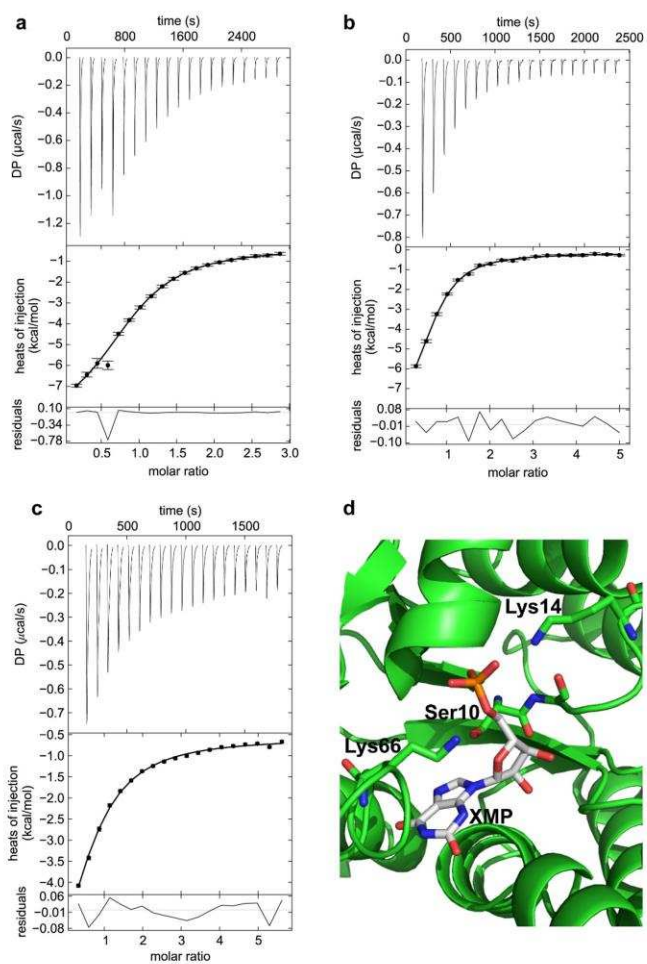


Figure 4

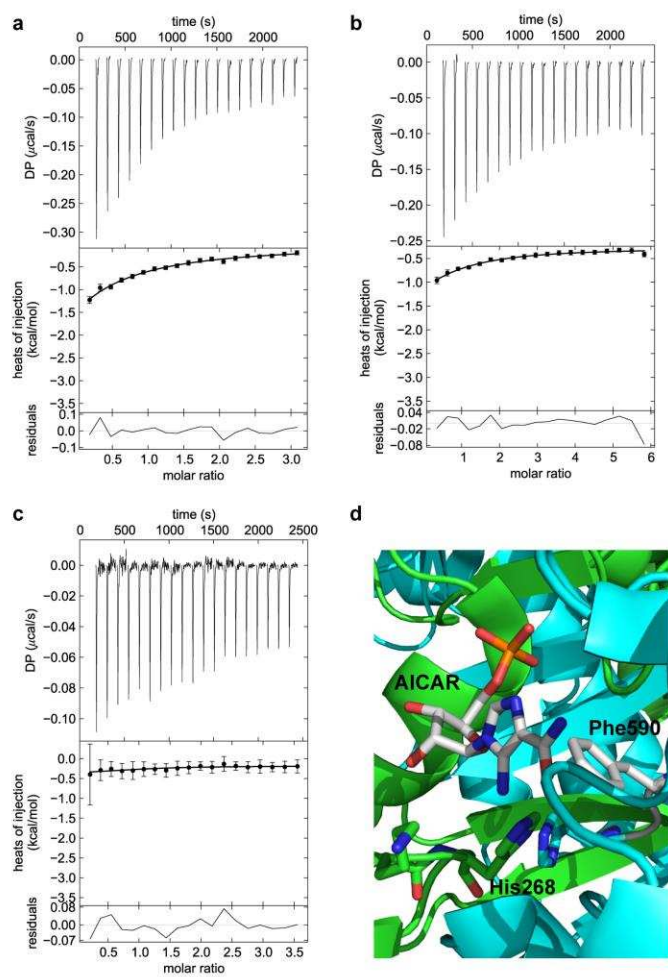


TABLE 1

Ligand	n	K_d [μ M]	ΔH / [kcal mol ⁻¹]	ΔG / [kcal mol ⁻¹]	ΔS / [cal mol ⁻¹ K ⁻¹]
AICAR	6	19.5 \pm 3.3	-9.7 \pm 0.6	-6.4 \pm 0.1	-10.9 \pm 2.1
PteGlu ₄	5	0.23 \pm 0.04	-12.6 \pm 0.1	-9.1 \pm 0.1	-11.8 \pm 0.6
PteGlu ₃	2	0.53 \pm 0.15	-10.8 \pm 0.3	-8.6 \pm 0.2	-7.5 \pm 1.2
PteGlu ₂	1	7.1 \pm 3.4	-9.44 \pm 1.3	-7.0 \pm 0.4	-8.1 \pm 4.3
10f-THF	1	132 \pm 12	-5.6 \pm 0.3	-5.3 \pm 0.1	-0.9 \pm 1.0
AMP	2	14.3 \pm 1.5	-6.6 \pm 0.3	-6.6 \pm 0.1	-0.1 \pm 1.1
AICAR in presence of AMP	2	32 \pm 21	-6.5 \pm 1.3	-6.1 \pm 0.4	-1.4 \pm 4.6
XMP (3-site binding model)	3	$K_{d1} = 1.4 \pm 0.3$ $K_{d2} = 55 \pm 7$ $K_{d3} = 7.0 \pm 1.1$	-4.9 \pm 0.1 16.7 \pm 0.1 -10.8 \pm 0.7	-8.0 \pm 0.1 -5.8 \pm 0.1 -7.0 \pm 0.1	10.3 \pm 0.5 75.5 \pm 0.6 (!) -12.6 \pm 2.5
XMP in presence of AICAR (2-site binding model)	1	$K_{d1} = 6.6 \pm 2.4$ $K_{d2} = 25 \pm 14$	-2.07 \pm 0.37 5.44 \pm 0.75	-7.1 \pm 0.2 -6.3 \pm 0.4	16.8 \pm 1.4 39.3 \pm 2.8 (!)

TABLE 2

Ligand	incA	K_d [μM]	ΔH / [kcal mol ⁻¹]
AICAR	0.27 ± 0.03	21.7 ± 5.0	-6.25 ± 0.79
IMP	0.37 ± 0.08	21.4 ± 11.2	-6.92 ± 1.13
XMP	0.14 ± 0.05 (incB)	12.7 ± 5.7	-5.02 ± 0.70

TABLE 3

Protein	AICAR		PteGlu ₄		AICAR (enzyme pre-treated with 100 μM PteGlu ₄)	
	K _d [μM]	ΔH [kcal mol ⁻¹]	K _d [μM]	ΔH/ [kcal mol ⁻¹]	K _d [μM]	ΔH/ [kcal mol ⁻¹]
ATIC-WT	19.5 ± 3.3	-8.5 ± 0.10	0.23 ± 0.03	-12.6 ± 0.1	94 ± 9	-3.6 ± 0.3
S10W	9.5 ± 1.0	-9.9 ± 0.56	0.078 ± 0.050	-11.6 ± 0.4	66 ± 18	-1.8 ± 0.15
S10W-F590A	34.1 ± 5.0	-10.3 ± 0.25	0.20 ± 0.04	-10.6 ± 0.1	No binding	No binding
S10W-F590I	62 ± 23	-3.3 ± 0.2	0.47 ± 0.12	-13.2 ± 0.3	No binding	No binding

Highlights

BINDING OF LIGANDS TO ATIC HAS BEEN STUDIED USING ISOTHERMAL TITRATION CALORIMETRY.

THE IMPCH AND AICARFT ACTIVE SITES EACH BIND PARTICULAR NUCLEOTIDES SELECTIVELY.

XANTHOSINE MONOPHOSPHATE SHOWS COOPERATIVE BINDING BETWEEN THE IMPCH ACTIVE SITES.

COOPERATIVE BINDING OF AICAR AND FOLATE LIGANDS IN THE AICARFT ACTIVE SITE WAS NOT OBSERVED.